PHYSICAL REVIEW B **77**, 094506 (2008)

Magnetization creep and decay in $YBa_2Cu_3O_{7-x}$ thin films with artificial nanostructure pinning

M. D. Sumption,[1] T. J. Haugan,[2] P. N. Barnes,[2] T. A. Campbell,[2] N. A. Pierce,[2] and C. Varanasi[3]
[1]*Department of Materials Science and Engineering, The Ohio State University, Columbus, Ohio 43210, USA*
[2]*Air Force Research Laboratory, Wright-Patterson Air Force Base, Dayton, Ohio 45433-7919, USA*
[3]*University of Dayton Research Institute, Dayton, Ohio 45469, USA*

(Received 11 June 2007; revised manuscript received 18 December 2007; published 7 March 2008)

Critical current and flux pinning have been studied for $YBa_2Cu_3O_{7-x}$ thin films with Y_2BaCuO_5 (211) precipitates introduced as layers and as random distributions. The 211 precipitates were introduced during pulsed laser deposition. In the case of the layered sample, the strata were spaced approximately 6.5 nm apart throughout the film thickness. Magnetically determined critical current density (J_c) was then fitted to $J_c \propto B^{-\alpha}$ above a magnetic field B^*, below which a relatively field independent $J_{c\text{-}self\text{-}field}$ was observed, consistent with previous results. Values of α were suppressed from the control sample values of $\alpha=0.5$ to lower values for pinned samples, reaching $\alpha=0.2$ for the layer pinned 211 sample at low temperatures. *M-H* was then measured as a function of ramp rate, and $U(J)$ vs J curves were extracted for temperatures from 4.2 to 77 K for pinned and control samples. Direct magnetization decay measurements were made for the 211 layer pinned sample, and good agreement was seen with ramp-rate-derived results. Using $U(J)=(U_0/\mu)[(J_c/J)^{\mu}-1]B^{-\nu}$, values of $\mu \cong 0.6-0.8$ were seen for all samples, while $\nu \cong 0.4$ for control samples, 0.1 for layer pinned samples, and 0.2–0.4 for the random pinned samples. The activation energy scale U_0 was 600–700 and 400 K for layer pinned and control samples, respectively, and 400–500 K for the random pinned samples. The values of μ and ν extracted were inconsistent with two dimensional pinning behavior in all cases, even though the layer spacing in the layer pinned sample is smaller than the calculated collective correlation length. While the layer pinned sample is clearly in the collective pinning regime, the artificial defects in the random pinned sample may be in the isolated strong pinning regime.

DOI: 10.1103/PhysRevB.77.094506 PACS number(s): 74.25.Qt, 74.25.Sv

I. INTRODUCTION

Studies of J_c, flux pinning, and vortex interactions in $YBa_2Cu_3O_{7-x}$ (YBCO) conductors have been extensive, being initiated shortly after the discovery of YBCO, and continuing today. Pinning in YBCO and HTSC in general has been analyzed within the context of the collective pinning model, as described in Blatter *et al.*[1] and underlying sources. Many researchers have investigated the implications of these ideas and the correspondence between theory and experiment using both direct transport and magnetization measurements of various forms. Measurements on powders and bulk samples have been complemented by recent measurements on coated conductors.

The transport properties of YBCO coated conductors and thin films have improved markedly in recent years. As part of the efforts to increase these properties, the thin film deposition and control techniques used to form them have been, in some cases, modified in order to create flux pinning defects within the structure of the sample. Some of the most interesting systems for analysis purposes are YBCO thin film samples with nanoinclusions of various kinds. These nanopinned structures can have notably improved J_c values, and the nanoinclusions can be imaged in TEM; examples of YBCO films with enhanced pinning include samples with 211 nanoparticle layers[2,3] or other nanostructures.[4–6] The exact way in which these nanoprecipitates or layers induced extra pinning is not clear, although it is suspected that at least in some cases the nanoinclusions are only indirectly responsible for the enhanced pinning. Taking first the case of the layer 211 samples, fully contiguous and uniform layers of suppressed order parameter would not contribute directly to pinning for fields perpendicular to the layers. Even though these layers are really pseudolayers with 5–20 vol % density of non-SC (superconducting) phase,[2] it is not clear whether the density and size of the nanoinclusions are sufficient for explaining the enhanced pinning. On the other hand, it may be that stress fields are induced [such as those observed in the transmission electron microscopy (TEM) images of Ref. 2] and that they accomplish the actual pinning. It has also been suggested[7] that if the 211 layers are sufficiently dense, they might cause a three dimensional (3D) to two dimensional (2D) transition, which optimizes the effectiveness of collective pinning by reducing the superconducting layer thickness below the collective pinning correlation length L_c^b.

Below, we will focus on the measurement of the flux pinning and dynamics in thin films of YBCO deposited by pulsed laser deposition (PLD) with and without 211 nanoparticulate pinning, added in the form of layers and random distributions, in an attempt to understand their character and dimensionality. In order to do so, the magnetic J_c for pinned and control samples was first measured. After this, both the ramp-rate variation of the *M-H* curves and direct measurements of the magnetization decay were used to investigate the $U(J)$ vs J curve, employing the interpolation expression to extract values of the pinning energy scale U_0 as well as the decay exponents.

II. THEORETICAL BACKGROUND

Pinning in YBCO conductors is usually analyzed in terms of the collective pinning model. This model, which assumes

TABLE I. Samples.

Sample	Other name	Type	Details	t (μm)	Film volume, (10^{-6} cm^3)	w (mm)
L211-A	TJ127	Layer 211	6.4 nm/1.28 nm:123/pin	0.269	2.76	3.25
Cont-A	TJ360	Control		0.301	2.80	3.13
R211-A	PV89	Random 211		0.884	8.95	3.18
R211-B	PV45	Random 211		0.417	4.06	3.26

the collective interaction of vortex bundles with pinning center distributions, makes general predictions about both J_c vs B and flux creep behavior. Used in the context of this and other models, the interpolation expression

$$U(J) = \frac{U_0}{\mu}\left[\left(\frac{J_c}{J}\right)^{\mu} - 1\right] \quad (1)$$

gives parameters that can be compared to predictions, where μ is the glassy exponent that varies with the dimensionality of the pinning and other particulars. In recent years, much of the work comparing experimental results to theoretical expectation has been in the context of the Bose glass theory[8] since columnar defects have been explored extensively.[9–11] In this regime, at low fields, one expects μ to be between 1/3 and 1, depending on whether the kink or superkink mode is operative.[1,9] For noncorrelated disorder at low fields in the single vortex regime, $\mu \approx 1/7$. Once in the collective regime, $\mu \approx 3/2$ at intermediate J_cs (small bundle), and at lower J_c (large bundle) $\mu \approx 7/9$. Measurements on YBCO have led to values of μ, which seem to be in agreement with this model, as seen in Refs. 12–15. In some cases, plastic pinning[16] is suggested to be responsible for fishtail effects and lower values of μ at higher values of J.[17] Miu *et al.*[18] claimed that plastic pinning leads to $\nu = \frac{1}{2}$, while Peurla *et al.*[19] claimed that the value is $\nu = 1$ for the collective pinning regime while going as $\frac{1}{2}$ in the plastic regime. However, the magnetic field values used in the present study (given the temperatures of measurement) are below the onset of the plastic regime.[17]

For models relating to 2D regimes, the situation seems less clear. The B dependence of $U(J)$ has been predicted to follow $U \propto \ln B$, and observed as such in Bi-2223 at higher temperatures in the decoupled state[20] as well as for YBCO with Pr-based non-SC interlayers,[21,22] $La_{0.3}Ca_{0.7}MnO_3$ interlayers,[23] and deoxygenated YBCO with a high intrinsic anisotropy.[24] On the other hand, the flux-flow creep model of Matsushita and co-workers[25,26] has predicted power law behavior with $\mu = 1$, $\nu = \frac{1}{2}$ for 2D and $\mu = 1/2$, $\nu = \frac{1}{4}$ for 3D. Additionally, it has been asserted[7,25] that $J \propto d^{-1/2}$, where d is the layer spacing.

Of course, there is a question about whether collective pinning is really applicable to these materials. Ijaduola *et al.*[27] pointed out that the isolated strong pinning theory of Ovchinnikov and Ivlev[28] predicts $U \propto J^{-\alpha}$, where $\alpha = 5/8$. Sauerzopf *et al.*[29] claimed that an $\alpha = \frac{1}{2}$ is an indication of direct summation, while $\alpha \cong 3$ is more consistent with collective pinning theories in the large bundle regime. Peurla[30] pointed out that in plastic pinning, $J \propto B^{-1/2}$.

III. EXPERIMENTAL ASPECTS

Three different types of films were prepared by pulsed laser deposition;[2,3] (a) layer 211, (b) random 211, and (c) a standard "control" sample (see Table I). The substrates were $LaAlO_3$ or $SrTiO_3$ single crystals, typically 3.2×3.2 mm^2. A lambda Physik LPX 305 KrF excimer laser ($\lambda = 248$ nm) was used to ablate a rotating target using a pulse repetition rate of 4 Hz (for all samples unless noted) with a laser fluence of ~ 3.2 J/cm^2. The oxygen pressure during the deposition was 300 mTorr (99.999% purity). The deposition temperatures were 775–780 °C. After deposition, an *in situ* oxygen anneal was performed at 500 °C for 30 mins.

The layer 211 sample was made by a sequential deposition of 123 layers and 211 nanoparticles by the ablation of separate 123 and 211 composition targets (under deposition conditions described previously[31]) using parameters chosen to optimize the superconducting properties of the 123 phase.[32] The 211 pseuso layer was approximately 1.3 nm thick and consisted of a high density (about 20 vol %) of 211 phase, with the remainder 123 phase. For the random 211 film samples, a special ablation target consisting of a thin sector (a 30° wedge) was attached with colloidal Ag paste on top of a YBCO target.[3] The target was rotated at a speed of 15–20 rpm, while the laser repetition rates were 4 Hz (R211-B) and 6 Hz (R211-A), yielding an approximately 11:1 ratio of YBCO:Y211 pulses during film growth. For layered samples, the preferred orientations of 211 and 123 cause a lattice mismatch (between the 211 and 123 phases) of 4.5%–7% in the a-b plane and $\cong 18\%$ along the c axis.[2] The orientation of 211 in randomly distributed films is presently unknown.[3] However, similar lattice mismatches on the order of 4%–18% are expected. The localized stress regions increase the size of the nonsuperconducting volume surrounding the defect and thereby change the pinning properties. Stress regions extending from the nanoparticles are observed mostly in the c-axis direction, consistent with the larger lattice mismatch in this direction.

A vibrating sample magnetometer (VSM) was used to extract magnetic J_c from thin film samples approximately 3 mm on a side. The VSM was calibrated with a Ni cylinder at room temperature with a known value of saturation magnetization. Measurements were corrected for sample size effects (the sensitivity function). Values of magnetization thus calibrated and the J_c's, which were extracted from them, were accurate to better than 5% (the lowest moment signal measurements, made at higher temperatures, are accurate to 5%). Temperatures were known to 0.1 K, and fields to 0.1 mT. Measurements were performed with the field paral-

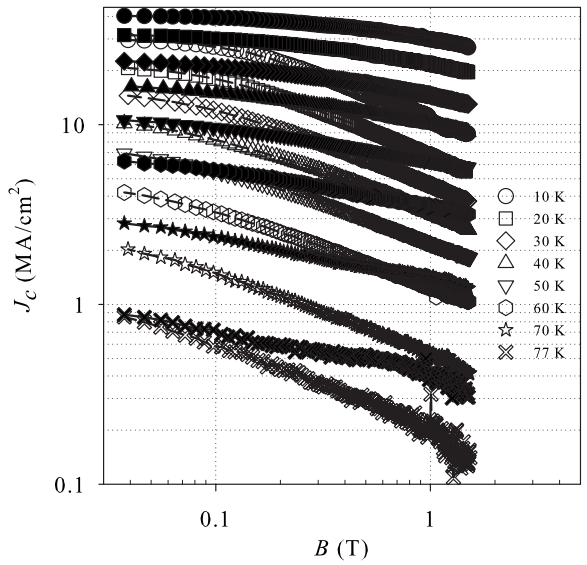

FIG. 1. Magnetic J_c at various temperatures for layer 211 pinned YBCO (L211-A) (filled) and control sample (Cont-A) (open).

lel to the c axis of the film, at temperatures ranging from 4.2 to 77 K, with ramp rates of 4–70 mT/s. J_c was calculated using the entire film thickness including pseudo-211 layers if present. Film thickness was determined by profilometry across acid-etched step edges on three to four areas of the film to reduce the standard error of the thickness below 5% (film thicknesses were typically 0.2–1 μm), and film widths were known to a level of 0.01 mm. The magnetically inferred J_c's of these square samples were estimated using a Bean model giving (in SI units, corrected for geometrical end effects)

$$J_c = \frac{2\Delta M}{w_1}\left[1 - \frac{w_1}{3w_2}\right]^{-1} \approx \frac{3\Delta M}{w}, \qquad (2)$$

where M is the magnetization and $w_1 \approx w_2 = w$ is the film width.[33,34] Here, $\Delta M = (M^+ - M^-)$, where M^+ is the trapping branch of the magnetization, and M^- is the shielding branch. For magnetic J_c determinations, the ramp rate was 70 mT/s. $\Delta M\ (H,T)$ was obtained at different ramp rates, and these data were used to determine $U(J)$ vs J, as described below. For L211-A, magnetization creep measurements were also taken at various temperatures for 100 mT, 300 mT, 500 mT, 700 mT, 900 mT, 1.1 T, and 1.3 T. For these measurements, the applied field was ramped to −1.7 T and then ramped to the measurement field (taking care to avoid overshoot); the magnetization creep measurements were then performed on the shielding branch.

IV. RESULTS AND DISCUSSIONS

A. Magnetic J_c and collective pinning lengths

Magnetic J_c for the layer 211 sample and the control sample were extracted from their associated M-H loops using Eq. (2), and the results are shown in Fig. 1. The usual low field region that varies slowly with $B < B^*$ is seen, along with a $J_c \propto B^{-\alpha}$, typically seen for these samples for $B > B^*$, as expected based on various pinning models. Here, we have defined B^* as its field at which the J_c reaches 95% of the low field (self-field) value. Whether B^* represents a crossover to single vortex behavior or merely defines a low field regime dominated by self-field effects can be debated. In any case, it usefully parametrizes the material. We note that while the J_{sf} for both samples is similar at 77 K, J_{sf} is larger for the layer pinned sample at all temperatures below this. Even more evident is the greatly reduced field dependence for the layer pinned sample in the power law regime; i.e., α is suppressed. The extracted values of B^*, α, and J_{sf}, each at 4 and 77 K, are given in Table II. J_c values were known to be better than 5%, as described in the experimental section. Typical R^2 values for the fits, which were used to extract α, were 0.995 or greater. For all measurements where B^* is quoted, the field resolution of the measurement is 1 mT; the error for our above defined B^* is similar based on our extraction procedure. Values of α for the control sample are about 0.5, at both 4.2 K and 77 K, while those of the layer 211 pinned sample are less than half of that. The B^* value has approximately doubled for the layer 211 pinned sample. These values can be compared to those for the random pinned 211 samples, also shown in Table II, with the J_c curves displayed in Fig. 2. For the random 211 samples, the α values are somewhat lower at 4.2 K, but not very different from that of the control sample at 77 K.

We can now calculate the longitudinal bundle correlation length for collective pinning, L_c^b. If the layer spacing or sample length is lower than L_c^b, 2D pinning is expected, at least within the collective pinning model. Gurevich[7] gave the

TABLE II. J_c, α, B^*, and L_c^b values.

Sample ID	J_{sf} (MA/cm^2) (4.2 K)	J_{sf} (MA/cm^2) (77 K)	L_c^b (nm) (4 K/0.1 T)	L_c^b (nm) (77 K/0.1 T)	B^* (mT) (4 K)	B^* (mT) (77 K)	α (4 K)	α (77 K)
Cont-A	31.9	1.56	100	450	60	[a]	0.49	0.43
L211-A	35.2	1.50	90	450	>135	8	0.16[b]	0.28
R211-A	40.1	1.05	90	550	140	6	0.25	0.48
R211-B	34.5	2.17	100	390	110	3	0.39	0.53

[a]Not enough low field data points were available to determine B^*, and the sample was damaged at a later point and could not be remeasured.
[b]10 K.

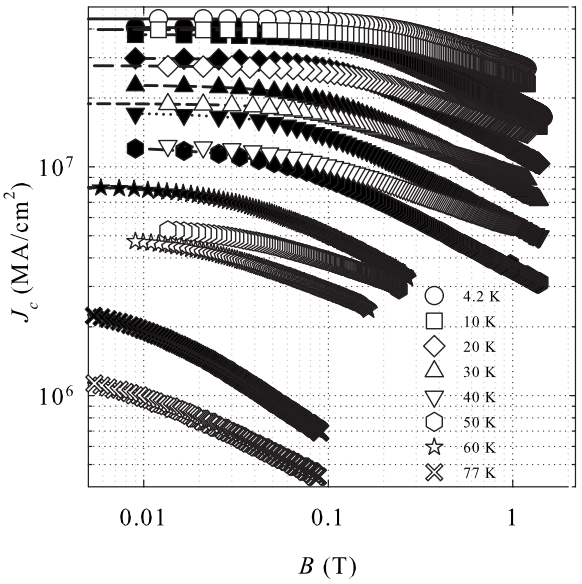

FIG. 2. Magnetic J_c at various temperatures for random 211 pinned samples R211-A (open) and R211-B (filled).

expression for this as $L_c^b\ (\mu\text{m}) = B^{1/4}\ (\text{T})/J^{-1/2}\ (\text{MA/cm}^2)$, with the condition of 2D pinning that $d < 2L_c^b$. Kimura *et al.*[25] gave the criterion for 2D pinning as the correlation length, L being greater than d, where L is given as

$$L = \left[\frac{(Ba_f)}{2\pi\mu_0 J_c}\right]^{1/2} = \frac{1}{\sqrt{2\pi\mu_0}}\frac{B^{1/4}\Phi^{1/4}}{J_c^{1/2}}$$
$$\approx 0.753\ \mu\text{m}\frac{B^{1/4}}{J_c^{1/2}(\text{MA/cm}^2)}. \quad (3)$$

These expressions have only a small constant factor difference; values for the longitudinal bundle correlation length as calculated for the expression from Ref. 7 are given in Table II for all samples. This estimate predicts that based on the relatively thin PLD sample thicknesses, all samples are in the 2D regime at 77 K, with the possible exception of R211-A, which would be 2D using the criterion of Gurevich[7] but not using the criterion of Kimura *et al.*[25] At 4.2 K, the sample length is three to eight times L_c^b, so the samples would be in the 3D regime on that basis. The distance between 211 layers for L211-A, however, would put it in the 2D regime at all temperatures if the layers were uniform enough to cause decoupling. However, these predictions do not seem to be borne out in the relaxation measurements, as described below. Similarly, transport measurements made as a function of applied field angle also suggest little anisotropy for this pinning contribution.[35] As noted above, the 211 layers are about 20% by volume 211, the remainder being a 123 phase. This lack of a contiguous and uniform layer of 211 is one possible reason why the pinning does not appear to be 2D in nature.

For the layer 211 sample, the 211 precipitate sizes are estimated[2] to be about 15 nm in diameter, with areal densities within the layers of about $2-5\times10^{11}$ particles/cm^2. Similar 211 precipitate sizes were seen for the random 211 samples,[3] with particles of an average diameter of 10 nm, an areal density of 1.7×10^{10}/cm^2, and a volume density of 2.2×10^{15}/cm^3. Porosity was also seen in the random 211 samples, with the pores being approximately 100–200 nm in size[3] and with volumetric densities of 2×10^{12}/cm^3. Since $\xi_{GL,a\text{-}b} \cong 1.5$ nm at 4.2 K and 3 nm at 77 K, respectively, these 211 precipitates are about five to ten times larger than $\xi_{GL,a\text{-}b}$. Additionally, strain fields are expected to emanate from them based on their lattice mismatch with the neighboring YBCO. The volume density of the 211 pinning sites alone, based on the above areal densities and the layer spacings, would reach 10^{24}/m^3, a relatively large number for "added" pinning centers. These numbers cannot be used in the context of the strong isolated pinning theory of Ovchinnikov and Ivlev[28] or van der Beek *et al.*;[36] they would lead to unphysical results because they are deposited in concentrated 2D layers. In the case of the random 211 samples, the theory can be tested using the form[36]

$$J_c = \frac{0.087N_i[D_iF(T)]^2}{\varepsilon}\left(\frac{\Phi_0}{B}\right)^{1/2}J_0 \quad (4)$$

for isolated strong pinning at intermediate field values. Here, N_i is the volumetric density of pinning sites, D_i is the length of the pins along the field direction, $F(T) = \ln[1 + D_i^2/(2\xi^2)]$ and J_0 is the depairing current density at zero temperature. Using the above value of N_i (2.2×10^{21}/m^3) and D_i (10 nm), along with $\xi_{GL,a\text{-}b}$ (4.2 K) $\cong 1.5$ nm, $\varepsilon = 1/5$, and $J_0 = 300$ MA/cm^2, we obtain $J_c \cong 13$ MA/cm^2 $B^{-1/2}$, with B in T. Since this value is within the range of modification seen with the random 211 additions, it is possible to consider these pins as directly responsible for the pinning, although this is far from clear. We can also consider the average distance between pinning centers by taking the cube root of the volume per defect, giving us a length of about 100 nm, which is close to the L_b^c value at low temperatures and is consistent with these defects acting in an individual rather than collective mode. As the temperature is increased, L_b^c grows, perhaps beginning to violate this condition. For the layer 211 samples, the density and layer spacings are such that we appear to be within the collective regime. For both layer and random 211 pinning samples, it may also be that the stress fields these defects induce are the true pinning centers.

B. Ramp-rate-derived magnetic relaxation measurements

M-H loop measurements were made for each sample at temperatures ranging from 4.2 to 77 K with varying ramp rates. We then used these data to extract the $U(J)$ vs J curves seen in Figs. 3–6, using an approach analogous to that of Maley *et al.*,[37] but for ramp-rate measurements. In order to do this, we used the approach of correlating the relaxation parameters to ramp rate seen, e.g., in Půst,[38] Jirsa and co-workers,[39–43] Půst,[44] and Reissner and Lorenz.[45] We will use the formulation of this approach given in Aruna *et al.*[46]

$$\frac{dH}{dt} + \frac{dM}{dt} = \left(\frac{2H\omega a}{R}\right)\exp\left(\frac{-U(J)}{kT}\right). \quad (5)$$

Here, ω is the characteristic attempt frequency, a is the hopping distance, R is the sample dimension, and $U(J)$ is the

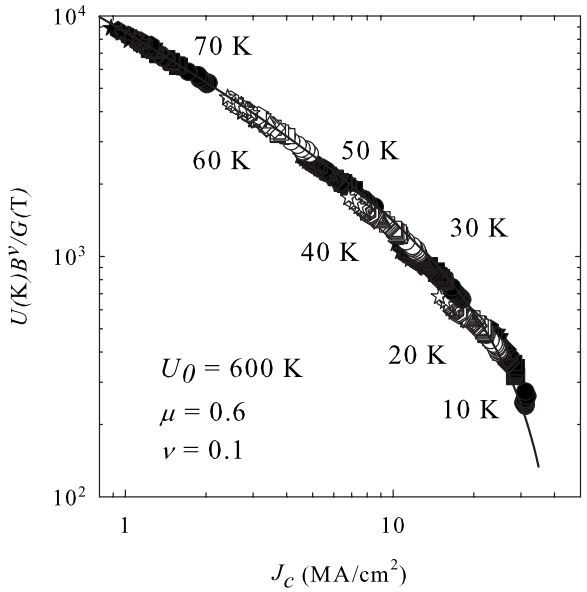

FIG. 3. Ramp-rate-generated $U(J)$ vs J for L211-A. Measurements are shown for 70, 60, 50, 40, 30, 20, and 10 K, symbols alternating filled and open, from left to right. At each temperature, measurements were made at 100 mT (●), 300 mT (■), 500 mT (◆), 700 mT (▲), 900 mT (▼), 1.1 T (■), and 1.3 T (★). U has been normalized to correct for temperature and field.

effective activation energy. This result is just that used by Maley *et al.*,[37] with the addition of a term describing the ramping of the field and the absence of a factor of π coming from sample geometry. The above expression is valid for cylinders[46] or disks[39] with fields along the symmetry axis. Since we are in a condition of continuous ramping, dM/dt can be neglected, and by looking at the variation of J (extracted from ΔM) vs dB/dt, we can obtain $U(J)$ vs J. We can, in analogy with Maley *et al.*,[37] take the natural log of both sides of Eq. (5) to get

$$\frac{U(J)}{k} = -T\,ln\,\frac{dB}{dt} + T\,ln\,\frac{B\omega a}{R}. \tag{6}$$

The units here are SI, and since the second term on the right hand side is a field dependent constant, we can proceed in parallel with the Maley approach, plotting the right hand side of Eq. (6) vs J for various temperatures and fields, setting the second term, $T\ln(B\omega a/R)$, equal to a constant (which we can denote as C, following Maley), chosen to give a best fit. In order to properly fit the data and to keep a physically sensible and temperature independent C, it is necessary to normalize $U(J)$ by a temperature dependent function $G(T)$ of, for example, the form $G(T)=[1-(T/T_c)]^n$, which incorporates the scaling of the intrinsic pinning parameters.[47] Tinkham[47] showed that the G-L theory predicted $n=3/2$ near T_c. Others[48] have used $G(T)=1-(T/T_c)^2$, while, on the other hand, McHenry *et al.*[49] demonstrated that $n=3/2$ works well over a wide temperature range. Shlyk *et al.*[13,17] made numerous measurements of magnetization decay in recently fabricated YBCO, and using a similar form, $G(T)=[1-(T/T_c)^2]^n$ has found fits using n ranging[13,17] from 1/2 to 3/2. In our fitting, we found the best results using the form of $G(T)$ from Shlyk *et al.*[17] with $n=3/2$, and used this expression in the results and analysis below.

Figure 3 shows the results for the layer pinned 211 sample. Temperatures from 10 to 77 K were measured, and ΔM was extracted at a variety of field values. The results were fitted to the interpolation expression above [Eq. (1)], after normalizing by $G(T)$, and a best fit was obtained for a $C=16$, $U=600$ K, $\mu=0.6$, and $\nu=0.1$, where $U(J)\propto B^{-\nu}$. These fits were evaluated by a criterion of continuity of the curve as determined by eye when varying C, U, J_{c0}, μ, and ν. Error estimates given in Table III are based on the sensitivity of the fit to the variation of the parameters. The observed value of μ for L211-A, interpreted within the context of the collective pinning model, suggests 3D pinning in the large bundle regime. The ν value is quite low—a value of $\frac{1}{4}$ is claimed by Kimura *et al.*[25] to be associated with a 3D behavior. The results of a similar analysis for the control sample is shown in Fig. 4. The extracted values for the various parameters are given in Table III, along with those of the layer 211 sample for comparison. Slightly lower U_0 values are seen for the control sample, while the μ factor is increased to 0.8. Most notable, however, is the ν factor, which has pushed up to 0.5. At lower temperatures, scaling was only possible when enhanced ν values of 0.6 and 0.9 were used at 10 and 4.2 K, respectively; possible reasons for this are discussed below. In any case, it is notable that the μ and ν factors for both control and layer 211 samples are consistent with 3D pinning if interpreted in the collective pinning model. The 2D collective pinning condition is expected to

TABLE III. Pinning energies and glassy exponent values.

Sample	U_0 (K)	μ	ν	v' (10 K)	v'' (4 K)	J_{c0} (MA/cm^2)	C
			Ramp-rate-derived data				
Cont-A	400 ± 50	0.80 ± 0.05	0.40 ± 0.05	0.6 ± 0.05	0.9 ± 0.05	36 ± 2	16 ± 1
L211-A	600 ± 50	0.60 ± 0.05	0.10 ± 0.05	0.10 ± 0.05		43 ± 2	16 ± 1
R211-A	400 ± 50	0.60 ± 0.05	0.20 ± 0.05	0.30 ± 0.05	0.60 ± 0.05	48 ± 2	16 ± 1
R211-B	500 ± 50	0.75 ± 0.05	0.40 ± 0.05	0.60 ± 0.05	0.80 ± 0.05	40 ± 2	16 ± 1
			Magnetization decay data				
L211-A	700 ± 50	0.65 ± 0.05	0.30 ± 0.05	0.30 ± 0.05	0.50 ± 0.05	39 ± 2	16 ± 1

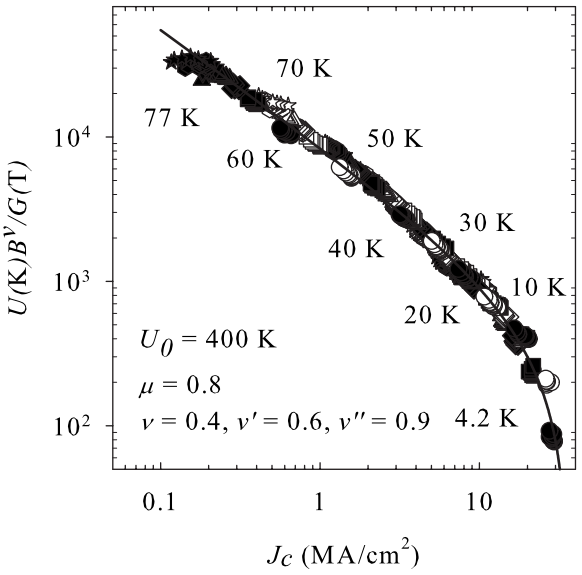

FIG. 4. Ramp-rate-generated $U(J)$ vs J for Cont-A. Measurements are shown for 77, 70, 60, 50, 40, 30, 20, 10, and 4.2 K, symbols alternating filled and open, from left to right. At each temperature, measurements were made at 100 mT (●), 300 mT (■), 500 mT (♦), 700 mT (▲), 900 mT (▼), 1.1 T (■), and 1.3 T (★). U has been normalized to correct for temperature and field.

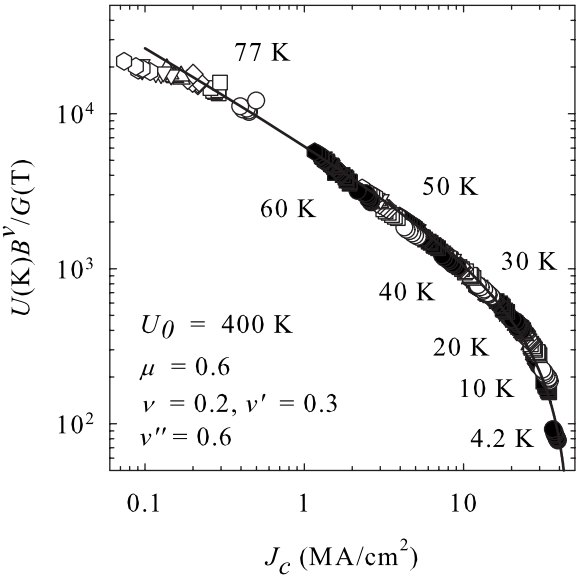

FIG. 5. Ramp-rate-generated $U(J)$ vs J for R211-A. Measurements are shown for 77, 70, 60, 50, 40, 30, 20, 10, and 4.2 K, symbols alternating filled and open, from left to right. At each temperature, measurements were made at 100 mT (●), 300 mT (■), 500 mT (♦), 700 mT (▲), 900 mT (▼), 1.1 T (■), and 1.3 T (★). U has been normalized to correct for temperature and field.

give $\ln B$ dependence, which none of these samples met. While the control samples could be considered to be "barely 2D" based on their near equivalence of d and L, the layer 211 samples would be well within the 2D regime if the 211 layers were truly decoupling the 123 layers, which would lead to a $\ln B$ dependence.[21–23] Thus, the layer 211 sample does not seem to be in the 2D regime.

The results for the random 211 pinned samples are shown in Figs. 5 and 6. These samples had U_0 values of 400 and 500 K for R211-A and R211-B, respectively. R211-A had μ and ν values close to L211-A, while R211-B had μ and ν values close to that of the control. Again, at the lowest temperatures, enlarged ν values were need to maintain scaling. On the basis of these parameters, R211-A behaved more similarly to the layer pinned sample, even though the absolute levels of J_c were lower in R211-A than in R211-B.

As mentioned above, it was necessary to use enlarged values of ν at lower temperatures to maintain scaling. A simple variation of C or changes in the G factor were unable to preserve scaling. The difficulty in maintaining scaling at these lower temperatures may be due to deviations from thermal activation. Various groups have noted the onset of quantum creep at lower temperatures,[50–55] as is expected. Both Landau and Ott[51,52] and Hoekstra *et al.*[50] found that the beginning of deviations from thermal activation may occur in the 10 K range (and Sefrioui *et al.*[55] below 5 K) for underdoped YBCO thin films. Whether it is present here for more optimally doped samples will require further detailed study.

C. Direct relaxation measurements on layer pinned YBCO

We have also performed direct relaxation measurements on the 211 layer pinned sample. Using the Maley approach[37] directly in this case, where $U=-kT\ln|dM/dt|+TC$, where for the present geometry $C=\ln(B\omega a/R)$, we plotted U/k vs J, finding a value of $C=16$, as shown in Fig. 7. U_0 was, in this case, 700 K, while $\mu=0.65$, as was previously seen for the ramp-rate measurements. The same temperature and field scaling factors $G(T)$ and $\nu=0.3$ were used ($\nu'=0.3$, $\nu''=0.5$).

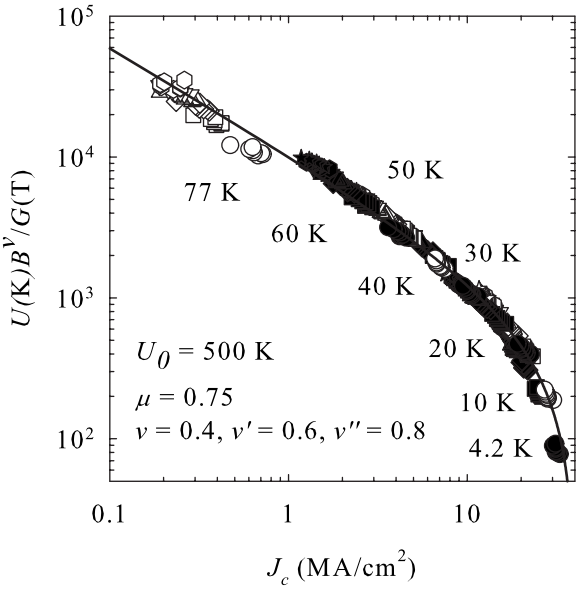

FIG. 6. Ramp-rate-generated $U(J)$ vs J for R211-B. Measurements are shown for 77, 70, 60, 50, 40, 30, 20, 10, and 4.2 K, symbols alternating filled and open, from left to right. At each temperature, measurements were made at 100 mT (●), 300 mT (■), 500 mT (♦), 700 mT (▲), 900 mT (▼), 1.1 T (■), and 1.3 T (★). U has been normalized to correct for temperature and field.

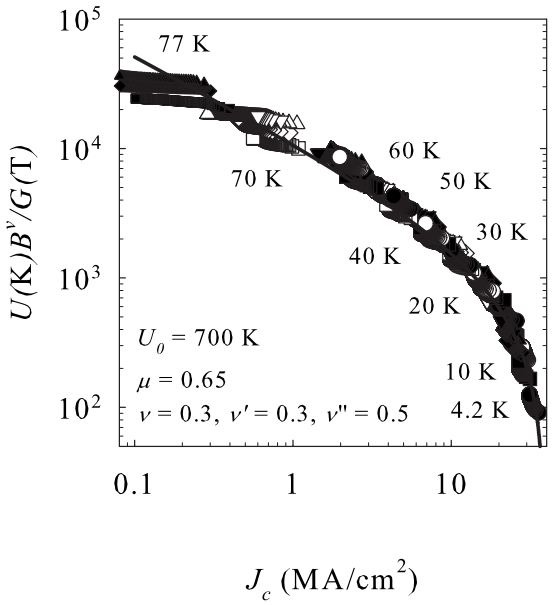

FIG. 7. Creep-drift-generated $U(J)$ vs J for L211-A. Measurements are shown for 77, 70, 60, 50, 40, 30, 20, 10, and 4.2 K, symbols alternating filled and open, from left to right. At each temperature, measurements were made at 100 mT (●), 300 mT (■), 500 mT (♦), 700 mT (▲), 900 mT (▼), 1.1 T (■), and 1.3 T (★). U has been normalized to correct for temperature and field.

These results are shown in Table III to be similar to those extracted from ramp-rate experiments described earlier.

In general, we see that the dependence of $U(J)$ on J as determined either by ramp-rate or direct measurements can be fitted to $U(J)=U_0/\mu[(J_c/J)^{\mu}-1]B^{-\nu}$, with results that are in agreement, and give values of μ and ν that are inconsistent with 2D pinning in the present 211 layer pinned samples. The dimensional character of the pinning increase is similar for random and layer 211 additions, suggesting that 3D pinning is operative in both cases. This is not surprising in view of the fact that the 211 layer has both 211 and 123 within it and, thus, may not act to cause the existence of 2D vortex segments within the layers and the associated 2D pinning increase. On the other hand, the exact microscopic origin of the pinning is not clear. In the case of the random 211 distributions, isolated strong pinning[28,36] are in reasonable agreement with the pinning increases observed. However, such expressions would not apply to the layer 211 samples. In addition, direct measurements have seen a lack of angular J_c variation (beyond the intrinsic levels),[35] suggesting that, at least in the layered case, it is not the 211 nanoparticles themselves that pin. It is possible that strain defects are induced by the subsequent 211 layer growth, possibly extending well into the 211 layer and forming a more 3D-like pinning network.

V. CONCLUSIONS

Magnetic J_c and magnetization decay have been measured for a set of YBCO thin film samples, which include layer pinned 211 samples, random 211 pinned samples, and control samples. The films were made via pulsed laser deposition, with 211 nanoparticles approximately 15 nm in diameter either concentrated in layers (stratum approximately 6.4 nm apart) or as a continuous and random distribution. Magnetic J_c curves were parametrized as $J \propto B^{-\alpha}$ above a relatively field independent region bounded by B^*. B^*. was seen to double with both layer and random 211 pinning. Values of α were pushed from 0.5 for the control sample down to 0.1 for the layer pinned 211 sample and were intermediate for the random 211 pinned samples. Magnetization decay measurements, both in the form of M-H loops taken at different ramp rates and direct decay measurements, were used to determine $U(J)$ vs J curves. $U(J)$ vs J response could be seen to properly scale at all fields and temperatures, fitting $U(J)=U_0/\mu[(J_c/J)^{\mu}-1]B^{-\nu}$, with appropriate choices of μ and ν. At the lowest temperatures, enlarged values of ν were needed.

Interpreting the results within the context of the collective pinning model, the values of μ and ν were consistent with a 3D behavior rather than a 2D behavior. While the overall sample thickness is large enough that the 2D regime is approached from the perspective of the sample thickness alone, these effects are not yet strong. The spacings of the layer pinned sample are well below the relevant collective pinning length. Thus, if the 211 layers were fully contiguous and uniform, a 2D behavior would be expected if longitudinal correlation length suppression was the main cause of additional pinning. However, the present data do not display a 2D signature. Thus, the 211 layers enhance pinning not by reducing the effective pinning correlation length, but by additional pinning, whether directly or (e.g., strain fields) indirectly.

ACKNOWLEDGMENTS

The Air Force Office of Scientific Research supported this work, both directly (AFRL) and via a summer research faculty program (Sumption). We would like to thank J. Thompson and A. Gurevich for clarifying discussions.

[1] G. Blatter, M. V. Feigel'man, V. B. Geshkenbein, A. I. Larkin, and V. M. Vinokur, Rev. Mod. Phys. **66**, 1125 (1994).
[2] T. Haugan, P. N. Barnes, R. Wheeler, F. Meisenkothen, and M. Sumption, Nature (London) **430**, 867 (2004).
[3] C. Varanasi, P. N. Barnes, J. Burke, J. Carpenter, and T. J. Haugan, Appl. Phys. Lett. **87**, 262510 (2005).
[4] K. Matsumoto, T. Horide, P. Mele, Y. Yoshida, M. Mukaida, A. Ichinose, and S. Horii, Physica C **426-431**, 1091 (2005).
[5] X. M. Cui, B. W. Tao, Z. Tian, J. Xiong, X. F. Zhang, and Y. R. Li, Supercond. Sci. Technol. **19**, 844 (2006).
[6] J. Hanisch, C. Cai, V. Stehr, R. Huhne, J. Lyubina, K. Nenkov, G. Fuchs, L. Schultz, and B. Holzapfel, Supercond. Sci. Technol.

19, 534 (2006).
[7] A. Gurevich, arXiv:cond-mat/0207526 (unpublished); see also, A. Gurevich, Supercond. Sci. Technol. **20**, S128 (2007).
[8] D. R. Nelson and V. M. Vinokur, Phys. Rev. B **48**, 13060 (1993).
[9] D. Niebieskikwiat, L. Civale, C. A. Balseiro, and G. Nieva, Phys. Rev. B **61**, 7135 (2000).
[10] L. Civale, Supercond. Sci. Technol. **10**, A11 (1997).
[11] P. N. Arendt, J. L. MacManus-Driscoll, M. P. Maley, and S. R. Foltyn, Appl. Phys. Lett. **84**, 2121 (2004).
[12] J. R. Thompson, Y. R. Sun, D. K. Christen, L. Civale, A. D. Marwick, and F. Holtzberg, Phys. Rev. B **49**, 13287 (1994).
[13] L. Shlyk, K. Nenkov, G. Krabbes, and G. Fuchs, Physica C **423**, 22 (2005).
[14] L. Shlyk, G. Krabbes, G. Fuchs, G. Stover, S. Gruss, and K. Nenkov, Physica C **377**, 437 (2002).
[15] D. X. Shen, A. M. Sun, C. F. Tian, H. Q. Bian, H. B. Zhu, Y. W. Li, and T. J. Chen, Physica C **432**, 1 (2005).
[16] Y. Abulafia, A. Shaulov, Y. Wolfus, R. Prozorov, L. Burlachkov, Y. Yeshurun, D. Majer, E. Zeldov, H. Wühl, V. B. Geshkenbein, and V. M. Vinokur, Phys. Rev. Lett. **77**, 1596 (1996).
[17] L. Shlyk, G. Krabbes, G. Fuchs, K. Nenkov, and B. Schüpp, J. Appl. Phys. **96**, 3371 (2004).
[18] L. Miu, E. Cimpoiasu, T. Stein, and C. C. Almasan, Physica C **334**, 1 (2000).
[19] M. Peurla, H. Huhtinen, and P. Paturi, Supercond. Sci. Technol. **18**, 628 (2005).
[20] M. Nideröst, A. Suter, P. Visani, A. C. Mota, and G. Blatter, Phys. Rev. B **53**, 9286 (1996).
[21] O. Brunner, L. Antognazza, J. M. Triscone, L. Mieville, and O. Fischer, Phys. Rev. Lett. **67**, 1354 (1991).
[22] F. Ichikawa, B. Zhao, T. Uchiyama, R. Kawabata, T. Koga, T. Arai, T. Fukami, T. Aomine, J. Sun, B. Xu, and L. Li, Physica C **264**, 275 (1996).
[23] V. Pena, Z. Sefrioui, D. Arias, C. Leon, J. Santamaria, and J. L. Martinez, J. Phys. Chem. Solids **67**, 387 (2006).
[24] Z. Sefrioui, D. Arias, M. Varela, C. Leon, and J. Santamaria, J. Alloys Compd. **323-324**, 572 (2001).
[25] K. Kimura, M. Kiuchi, E. S. Otabe, T. Matsushita, S. Miyata, A. Ibi, T. Muroga, Y. Yamada, and Y. Shiohara, Physica C **445-448**, 141 (2006).
[26] T. Matsushita, T. Watanabe, Y. Fukumoto, K. Yamauchi, M. Kiuchi, E. S. Otabe, T. Kiss, T. Watanabe, S. Miyata, A. Ibi, T. Muro, Y. Yamada, and Y. Shiohara, Physica C **426-431**, 1096 (2005).
[27] A. O. Ijaduola, J. R. Thompson, R. Feenstra, D. K. Christen, A. A. Gapud, and X. Song, Phys. Rev. B **73**, 134502 (2006).
[28] Y. N. Ovchinnikov and B. I. Ivlev, Phys. Rev. B **43**, 8024 (1991).
[29] F. M. Sauerzopf, M. Zehetmayer, A. K. Shler, and H. W. Weber, Physica C **341-348**, 1271 (2000).
[30] M. Peurla, H. Huhtinen, and P. Paturi, Supercond. Sci. Technol. **18**, 628 (2005).
[31] T. Haugan, P. N. Barnes, I. Maartense, C. B. Cobb, E. J. Lee, and M. Sumption, J. Mater. Res. **18**, 2618 (2003).
[32] T. Haugan, P. Barnes, L. Brunke, I. Maartense, and J. Murphy, Physica C **297**, 47 (2003).
[33] E. M. Gyorgy, R. B. van Dover, K. A. Jackson, L. F. Scheneemeyer, and J. V. Waszczak, Appl. Phys. Lett. **55**, 283 (1989).
[34] S. Hu, H. Hojaji, A. Barkatt, M. Boroomand, A. N. Thorpe, and S. Alterescu, Phys. Rev. B **43**, 2878 (1991).
[35] L. Civale and B. Maiorov (unpublished).
[36] C. J. van der Beek, M. Konczykowski, A. Abal'oshev, I. Abal'osheva, P. Gierlowski, S. J. Lewandowski, M. V. Indenbom, and S. Barbanera, Phys. Rev. B **66**, 024523 (2002).
[37] M. P. Maley, J. O. Willis, H. Lessure, and M. E. McHenry, Phys. Rev. B **42**, 2639 (1990).
[38] L. Půst, Supercond. Sci. Technol. **5**, 497 (1992).
[39] M. Jirsa, L. Půst, H. G. Schnack, and R. Griessen, Physica C **207**, 85 (1993).
[40] A. A. J. Van Dalen, M. R. Koblischka, R. Griessen, M. Jirsa, and G. Ravi Kumar, Physica C **250**, 265 (1995).
[41] L. Půst, D. Dlouhý, and M. Jirsa, Supercond. Sci. Technol. **9**, 814 (1996).
[42] M. Jirsa, T. Nishizaki, N. Kobayashi, M. Muralidhar, and M. Murakami, Phys. Rev. B **70**, 024525 (2004).
[43] A. Yu. Galkin, L. Půst, M. Jirsa, P. Nálevka, and M. R. Koblischka, Physica C **308**, 21 (1998).
[44] L. Pust, Supercond. Sci. Technol. **3**, 598 (1990).
[45] M. Reissner and J. Lorenz, Phys. Rev. B **56**, 6273 (1997).
[46] S. A. Aruna, H. M. Shao, J. C. Shen, Y. Rui, H. L. Ji, X. N. Xu, and X. X. Yao, Physica C **341-348**, 1153 (2000).
[47] M. Tinkham, Phys. Rev. Lett. **61**, 1658 (1988).
[48] E. V. Blinov, H. Huhtinen, E. Lahderanta, Yu. Stepanov, K. Traito, and P. Varjonen, Physica C **334**, 115 (2000).
[49] M. E. McHenry, S. Simizu, H. Lessure, M. P. Maley, J. Y. Coulter, I. Tanaka, and H. Kojima, Phys. Rev. B **44**, 7614 (1991).
[50] A. F. Th. Hoekstra, A. M. Testa, G. Doornbos, J. C. Martinez, B. Dam, R. Griessen, B. I. Ivlev, M. Brinkmann, K. Westerholt, W. K. Kwok, and G. W. Crabtree, Phys. Rev. B **59**, 7222 (1999).
[51] I. L. Landau and H. R. Ott, Physica C **340**, 251 (2000).
[52] I. L. Landua and H. R. Ott, Physica B **284**, 791 (2000).
[53] T. Stein, G. A. Levin, C. C. Almasan, D. A. Gajewski, and M. B. Maple, Phys. Rev. B **61**, 1538 (2000).
[54] T. Stein, G. A. Levin, C. C. Almasan, D. A. Gajewski, and M. B. Maple, Phys. Rev. Lett. **82**, 2955 (1999).
[55] Z. Sefrioui, D. Arias, F. Morales, M. Varela, C. Leon, R. Escudero, and J. Santamaria, Phys. Rev. B **63**, 054509 (2001).